ARTICLE IN PRESS

International Journal of Biological Macromolecules xxx (xxxx) xxx

ELSEVIER

Contents lists available at ScienceDirect

International Journal of Biological Macromolecules

journal homepage: www.elsevier.com/locate/ijbiomac



Thermal – chemical - mechanical characterization of *Anacardium occidentale* tree gum

Jebaratnam Joy Mathavan a, Muhammad Hafiz bin Hassan b

- a Department of Engineering Technology, Faculty of Technology, University of Jaffna, Kilinochchi premises, Ariviyal Nagar, Kilinochchi 44000, Sri Lanka
- ^b School of Mechanical Engineering, Engineering Campus, Universiti Sains Malaysia, 14300 Nibong Tebal, Pulau Pinang, Malaysia

ARTICLE INFO

Keywords: Anacardium occidentale tree gum μ X-ray fluorescence test Simultaneous thermal analysis

ABSTRACT

Anacardium occidentale (cashew) tree gum is being used in several sectors, including the pharmaceutical sector. This gum has been explored more in the medical field by many previous researchers, but there is a big research gap regarding its thermal and mechanical properties. Therefore, this research is intended to reveal the thermal, chemical, and mechanical characteristics of Anacardium occidentale tree gum. The results obtained in this regard are then compared with certain properties of artificial resins. Thermal analysis is carried out using a thermogravimetric analyzer, and differential scanning calorimeter, elemental analysis is carried out using a scanning electron microscope and a micro-X-ray fluorescence analyzer; and mechanical tests are carried out using a nano-indentation tester and a universal testing machine. The pH of 4.76 shows that the gum is acidic in nature, and the peaks obtained from thermal analysis demonstrate that it doesn't have a melting point. The microhardness value, tensile strength, flexural strength, and compressive strength of cashew gum are 218.39 MPa, 1.667 MPa, 3.64 MPa, and 2.667 MPa, respectively. The obtained results show that, Anacardium occidentale tree gum has comparable thermal properties to those of artificial resins and other natural gums.

1. Introduction

Plant gums are produced either as exudates, seed gums, seaweed gums, or pectin [1]. Many tropical plants produce gum as exudates, and these include *Acacia senegal, Anacardium occidentale* L., and *Khaya senegalensis* [1,2]. Gummy exudates are produced by a process called gummosis which is the secretion of gluey substances from plant stem and trunk. The sticky substance, on exposure to air, solidify to form amorphous translucent solid called gum [3]. Natural gums are hydrocarbons of high molecular mass. Artificial gums are petroleum products, rubber latex synthetic polymeric gums, balms and resins. The term 'natural gum', refers to plant or microbial polysaccharides and their derivatives that are capable of forming dispersions in cold or hot water, producing viscous mixtures or solutions. In other words, the term gum means soluble cellulose derivatives and those derived from, and modifications of, other polysaccharides that, in their original (natural form), would be insoluble [4].

Anacardium occidentale (cashew tree) produce cashew gum, and it is hydrophilic in nature. The hydrolysis of the cashew gum results in a higher galactose content and other constituents such as arabinose, glucose, rhamnose, mannose, xylose, and glucuronic acid [5,6]. Cashew

gum is a complex polysaccharide of high molecular mass around 9,500,000. It occurs as a partially acetylated derivative. The gum is composed of complex branched hetero-polysaccharides and their calcium, magnesium, potassium and sodium salts [4]. It is bio-degradable as well as bio-compatible, in nature [2]. Exudates are generally produced by wounding the tree during pruning or as a direct result of attack by insects or microorganisms. As like many other polysaccharides including gum arabic, acacia gum and khaya gum; cashew gum also can be used in the pharmaceutical and cosmetic industries, as an agglutinant for capsules and pills, and in the food industry as a stabilizer of juices, beer and ice cream, and also, it can be utilized in the making of cashew wine [4,7-9]. Cashew gum is not only good adhesives, but also contain a small amount of cashew oil, which can be used as an insect repellent or as a lubricant in the electrical insulation of aero planes [4]. The present study addresses a significant research gap by focusing on the thermal and mechanical properties of Anacardium occidentale (cashew) tree gum, which has been relatively unexplored compared to its applications in the pharmaceutical sector. This highlights the novelty and importance of the research.

E-mail address: joymathavan2013@gmail.com (J.J. Mathavan).

https://doi.org/10.1016/j.ijbiomac.2024.132396

Received 4 March 2024; Received in revised form 7 May 2024; Accepted 13 May 2024

0141-8130/© 2024 Elsevier B.V. All rights are reserved, including those for text and data mining, AI training, and similar technologies.

Please cite this article as: Jebaratnam Joy Mathavan, Muhammad Hafiz bin Hassan, *International Journal of Biological Macromolecules*, https://doi.org/10.1016/j.ijbiomac.2024.132396

^{*} Corresponding author.

2. Methodology

The study employs a variety of analytical techniques, including thermal analysis (thermogravimetric analyzer, differential scanning calorimeter, and simultaneous thermal analyzer), elemental analysis (Fourier transform infra-red spectrometer, scanning electron microscope and micro-X-ray fluorescence analyzer), and mechanical tests (nano-indentation tester and universal testing machine). This comprehensive approach ensures a thorough understanding of the gum's properties.

2.1. Gum extraction and preparation

Crude exudates from cashew trees (Anacardium occidentale) were manually collected in Western province of Sri Lanka, followed by a thorough cleaning process to remove bark particles and other foreign materials by hand. Subsequently, an equal weight of regular water was added, and the mixture underwent homogenization using a blender. After blending, the solution was left undisturbed for 24 h to ensure complete dissolution. The resulting solution was filtered through a sieve to eliminate any external particles or mucilage, and then left to thicken under ambient temperature and humidity. A portion of the material was powdered as needed for specific tests, while another portion was utilized for mechanical testing. This latter portion was transferred to a mold measuring 20 cm \times 10 cm, with a mold release sheet at the bottom. The material was allowed to naturally air-dry at ambient temperature and was subsequently cut into various sizes according to the specifications of the tests. It's important to note that the properties of gums derived from trees of different age groups, locations, climatic zones, soils may vary and this factor is a limitation in this study. But the literature studies and comparisons in the following sections shows that these variations are not significant.

2.2. Determination of pH

A 2 g gum sample was dispersed in an ample amount of deionized water, and additional deionized water was added to achieve a volume of 100 ml, resulting in a 2 % $^{w}/_{v}$ polymer dispersion. The pH of the dispersion was measured 24 h after preparation using a pH meter supplied by EUTECH INSTRUMENTS.

2.3. Thermogravimetric analysis

Thermal stress often leads to the degradation of most polymers, whether synthetic or natural [10]. This degradation is ascribed to processes like chain depolymerization, point splits, or the elimination of low molecular weight fragments, resulting in mass loss as temperatures increase [11]. These thermal effects involve physical or chemical changes and are associated with thermodynamic events [10]. Techniques such as thermogravimetry (TG), derivative thermogravimetry (DTG), differential thermal analysis (DTA), and differential scanning calorimetry (DSC) are employed to measure changes in energy and mass. These analytical methods provide valuable insights into alterations in crystalline structure, reaction kinetics, melting and boiling points, glass transition, and other relevant properties [12].

The TG analysis was conducted using a Pyris 1 TGA Thermogravimetric Analyzer from PerkinElmer Life and Analytical Sciences. The instrument boasts a temperature range up to $1000~^\circ\text{C}$, scanning rate of $0.1~^\circ\text{C/min}$ - $200~^\circ\text{C/min}$, temperature precision of $\pm 2~^\circ\text{C}$, temperature accuracy of $\pm 0.1~^\circ\text{C}$, balance sensitivity of $0.1~\mu\text{g}$, and balance precision of 0.001~%. The analyses involved an 8.1~mg weighed sample in a nitrogen atmosphere with a flow rate of 20 ml/min. A heating rate of $20~^\circ\text{C/min}$ was applied, ranging from $30~^\circ\text{C}$ to a final temperature of $900~^\circ\text{C}$.

2.4. Differential scanning calorimetry

In a Differential Scanning Calorimetry (DSC) instrument, the sample and a reference are held in designated holders, and the temperature is steadily increased. The heat exchange between the sample and the reference is measured, facilitating the detection of processes occurring in the sample as it heats up from ambient temperature to its decomposition point [13]. For the DSC experiment, the DSC Q20 V24.11 equipment from TA Instruments was utilized here. The instrument features a temperature range up to 725 °C, temperature accuracy of ± 0.1 °C, temperature precision of ± 0.05 °C, heating rate up to 200 °C/min, dynamic measurement range of ± 350 mW, and sensitivity of 1 μ W. A sample weight of 6.66 mg was employed under a 50 ml/min nitrogen flow, with a heat flow rate of 10.00 °C/min to achieve a temperature range of 320.00 °C.

2.5. Simultaneous thermal analysis (STA)

Simultaneous Thermal Analysis (STA) is an analytical technique that concurrently measures both thermogravimetry (TG) and differential thermal analysis (DTA). To validate the outcomes derived from TGA and DSC analyses, a real-time examination of sample changes with rising temperature was performed through STA. The Simultaneous Thermal Analyzer STA8122, manufactured by Rigaku Corporation, was employed under static air conditions to observe and analyze alterations in the sample within the ambient environmental setting. Testing was conducted with preset parameters, including a maximum temperature of 400 $^{\circ}$ C and a temperature increasing rate of 20 $^{\circ}$ C/min. The sample observation feature in TG-DTA allows for measurements while capturing visual images of the sample using a CCD camera. These images provide valuable insights into shape changes or color variations in the sample associated with a reaction, enhancing the interpretation of TG-DTA results.

2.6. Fourier transform infra-red spectrometry (FTIR)

The FTIR analysis utilized the 400 Spotlights FTIR Imaging System integrated with an Attenuated Total Reflection (ATR) model from PerkinElmer, USA, for Mid-NIR infrared analysis. Zinc Selenide detector is employed to detect the spectra transmission within a scan range from $600~{\rm cm}^{-1}$ to $4000~{\rm cm}^{-1}$, using a resolution of $8~{\rm cm}^{-1}$ for 16 scans. The IR spectrum software version 10.3.2 by PerkinElmer is used for spectrum processing. ATR is a highly reliable IR sampling technique that ensures excellent data quality along with optimal reproducibility.

2.7. Scanning electron microscopic imaging

The Scanning Electron Microscope (SEM) S-3400 N, provided by Hitachi Science Systems, Ltd., was employed to observe magnified images of the powdered sample. The SEM offers magnification capabilities ranging from $5\times$ to $300,000\times$, an acceleration voltage between 0.3~kV to 30~kV, and a vacuum pressure of 1.5×10^{-3} Pa. The electron source utilizes a pre-centered cartridge type tungsten hairpin filament. The sample is affixed to the sample stage using double-sided adhesive tape and inserted into the SEM for imaging. Following image acquisition, EDAX is utilized to scan the image under the "area scanning" option to identify the elements present at specified points of interest.

2.8. Micro X-ray fluorescence test

Micro X-ray Fluorescence (μ -XRF) is an analytical technique employed to ascertain the elemental composition of materials at a microscopic scale. A notable advantage of micro XRF is its non-destructive nature. Beyond elemental analysis, it can generate elemental maps of samples, offering insights into the distribution of elements within the sample. The μ -XRF instrument used in this study was

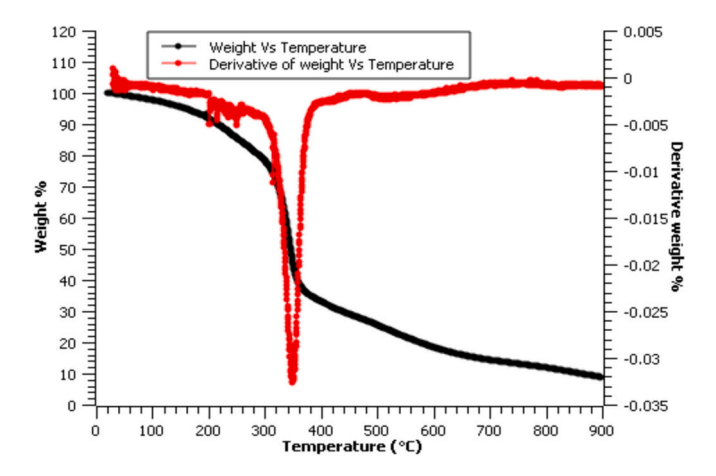


Fig. 1. Thermogravimetric curves obtained for the cashew gum sample.

the M4 Tornado, manufactured by Bruker Nano GmbH in Berlin, Germany. A Rhodium tube was utilized to emit X-rays, with a supply of 40 kV and 600 mA, and a pressure of 2 mbar during experimentation. The sample was positioned and adjusted to achieve a clear focus image and a high concentration of X-ray beam scattering. The instrument can test samples with thicknesses ranging from 400 nm to 20 μ m in metallic samples, 4.5 μ m to 3 mm in glass, stone, or ceramic samples, and 10 μ m to 2 cm in plastic or wood samples, based on the photon energy supply ranging from 1.7 keV to 25.5 keV.

2.9. Determination of micro hardness

The micro hardness test employed a Nano Test Vantage machine manufactured by Micro Materials Ltd. The sample was allowed to thermally stabilize in the instrument for approximately 30 min as per the manual. It was essential for the experimentation sample to possess a fine surface finish and be free from any dirt or grease, as these irregularities could impact the readings. Loading and unloading curves were obtained, and the hardness value was determined for subsequent analysis. The nano indentation test incorporated the following experiment parameters: a maximum load of 500 mN, minimum load of 50 mN, limit stop

load of 0.01 mN, initial load of 0.01 mN, loading and unloading rate of 5.0 mN/s, 6 s dwell at maximum load in one column containing 10 indentations, with a Z offset of 0 μm and Y offset of 15 μm , and a retraction distance of 15 μm .

2.10. Determination of tensile strength

Tensile test was conducted in accordance with ASTM D638, utilizing specimens in the dog bone shape with dimensions of 12.7 mm width, 165 mm length, and 3.2 mm thickness. The test was performed on a computerized universal testing machine, specifically the INSTRON 3367 model supplied by GT INSTRUMENTS SDN. BHD, with a capacity of 400 kN. The rate of crosshead movement was set at 1.5 mm/min. Graphical representations were generated for the tensile test outcomes, including ultimate strength, yield strength, and percentage elongation of the specimen. The dimensions and displacement rate (1.5 mm/min) were input into the software, and then the test was conducted. The test data results were subsequently converted to various tensile properties such as tensile strength, strain, and elastic modulus. Various other researchers also have used ASTM D638 for tensile testing of composite resins [14,15].

2.11. Determination of flexural strength

In accordance with ASTM D790-17, the flexural test was conducted using specimens with a thickness of 3.2 ± 0.3 mm, a span length of 16 ± 1 times that of the thickness, and a width less than one fourth of the span length (12.7 mm width, 127 mm long, 3.2 mm thickness). The rate of crosshead movement was set at 1.5 mm/min, and the maximum limiting deflection was set at 40 mm. The graph generated from the test provided values for maximum load, maximum extension, flexural stress, flexural strain, and modulus. Graphs depicting load vs. extension and flexural stress vs. flexural strain were then plotted. It is noteworthy that various other researchers have also employed ASTM D790 for flexural testing of composite resins [16,17].

2.12. Determination of compressive strength

To determine the compressive strength, compressive yield point, and modulus of the resin, ASTM D695 standards were followed.

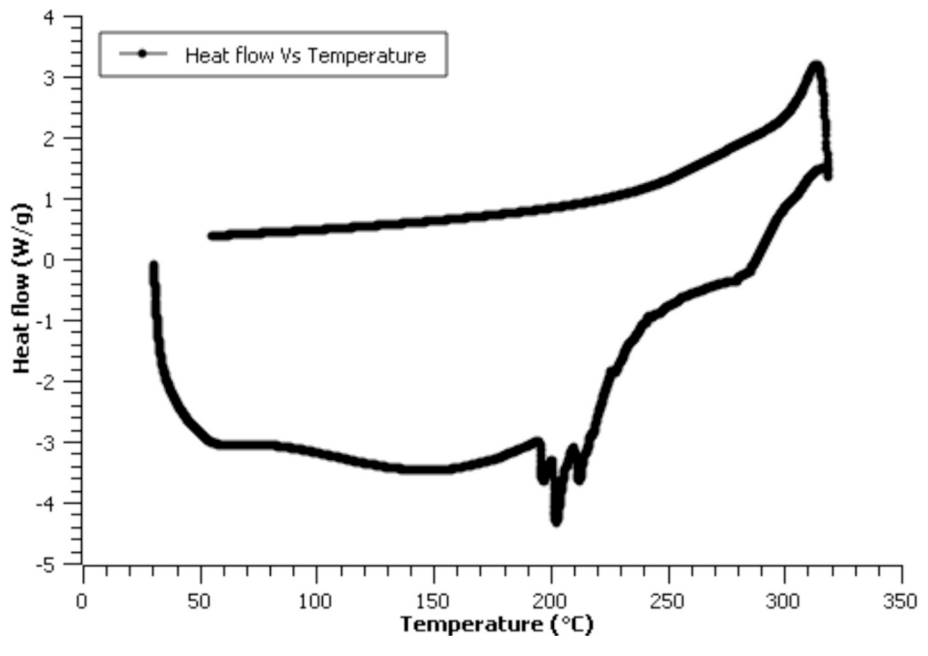


Fig. 2. Differential scanning calorimetry curves obtained for the cashew gum sample.

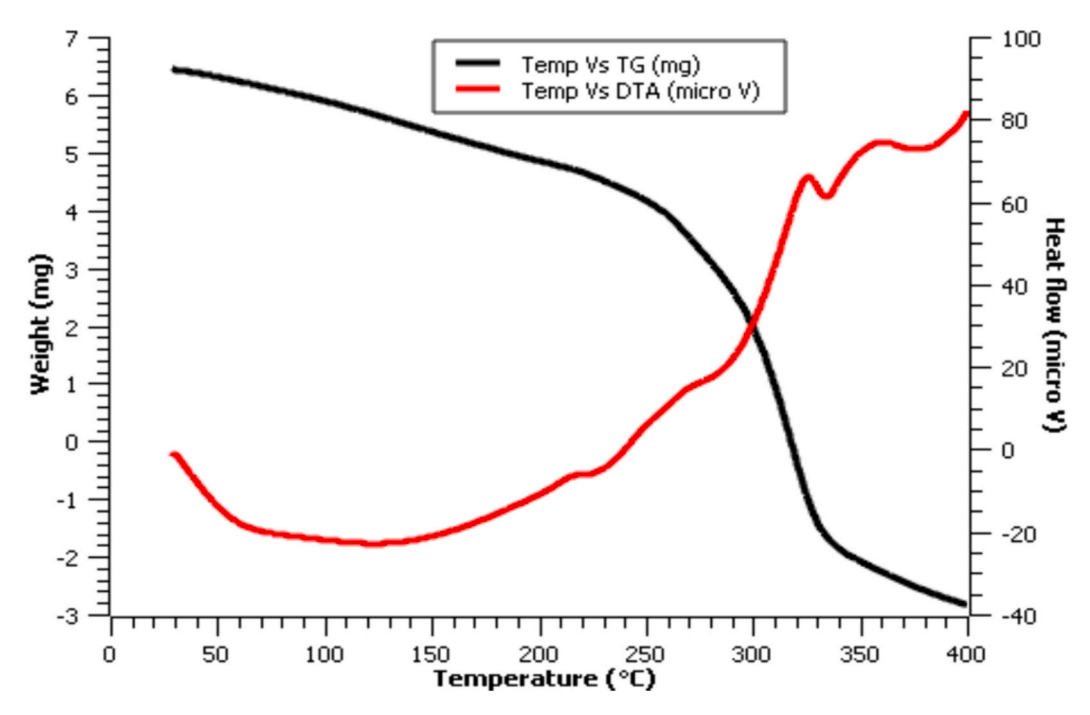


Fig. 3. TG-DTA curve obtained under static air condition.

Compression tests were performed on samples measuring 12.7 mm in width, 25.4 mm in length, and 12.7 mm in thickness. The tests were conducted with a cross-head movement of 1.5 mm/min and a specified maximum compression of 50 % of the length of the sample. It is noteworthy that the same Universal Testing Machine (UTM) with different heads was utilized for each of the tensile, flexural, and compression tests.

2.13. Viscosity and electrical resistivity

Viscosity and electrical resistivity were measured with changing temperature from 30 °C to 90 °C and concentrations of 10, 20, 30 40, and $50\%^{\text{W}}/_{\text{V}}$ of the gum. For example, $10\%^{\text{W}}/_{\text{V}}$ means 10 g of gum for 90 ml of water. The viscosities of the gum dispersions were obtained at shear rate of 100 rpm using Brookfield viscometer version 5 spindle 2 (Brookfield Engineering Labs, Stoughton, USA) according to Eshun et al. [18]. A 3 min standardization was done before the reading of viscosities was taken [19]. In general, viscosity of gums depends on the type of gum, temperature, concentration, pH, and the presence of other substances in the solution. The effect of these individual factors on viscosity varies from gum to gum [18]. A graph of the viscosities against concentration was plotted to evaluate the effect of the increase in concentration on the viscosity.

3. Results and discussion

3.1. pH value

The pH value obtained for cashew gum in the current study, at a concentration of 2 % w/v, is 4.76. This falls within the specified interval of 3.8 to 5.22 according to Gyedu-Akoto et al. [20]. It's important to note that the pH of gums derived from trees of different age groups and locations can vary [20]. In a similar way, another research group reported a pH value of 4.04 for cashew gum, aligning with the comparable range of khaya gum (pH = 3.38–4.2) [21,22], and acacia gum (pH = 4.61) [22].

3.2. Thermo gravimetric analysis

The thermogravimetric curves of the samples are depicted in Fig. 1. The initial stage, up to 195 °C, is attributed to moisture evaporation, resulting in a mass loss of 7.61 %. Subsequently, the decomposition of the three biomass lignocellulosic components occurs. Hemicellulose is the first to decompose between 201 °C and 296 °C, with a mass loss of 12.87 %, followed by cellulose between 300 °C and 391 °C, with a mass loss of 44.2 %. Lignin, being the component with the most complex structure, undergoes decomposition over a wide range [23], from 400 °C up to high temperatures, such as 900 °C, with a residual mass at 900 °C amounting to 8.86 %. The thermal decomposition stages of hemicellulose between 200 and 300 °C, followed by cellulose between 250 and 380 °C, along with water vaporization between 50 and 150 °C, have also been reported by [24–26]. These stages are evident in the DTG curve, showing peaks at 258 °C (related to hemicellulose) and 340 °C (associated with cellulose decomposition in cashew gum). Some researchers have reported decomposition temperatures of 262 °C and 314 °C for cashew tree gum [9].

Cellulose exhibits the highest activation energies among the compounds. This is attributed to the fact that cellulose is an extended polymer of glucose units without any branches [24]. In contrast, hemicellulose has a randomly branched amorphous structure, leading to a lower activation energy. This is the reason why hemicellulose decomposes more readily at lower temperatures [27]. Lignin, with its highly complex structure comprising three types of heavily crosslinked phenylpropane structures [24], has an activation energy lower than that of hemicellulose and cellulose, indicating easier thermal degradation. However, lignin presents much lower values of pre-exponential factors, resulting in a lower reaction rate. This characteristic is reflected in the broad temperature range over which its degradation occurs and the high temperature required for complete degradation.

Cashew gum, being a complex heteropolysaccharide, undergoes thermal decomposition through a mechanism that is not fully understood. Typically, the process involves dehydration, depolymerization, decarbonylation, and pyrolytic decomposition, leading to the evolution of H_2O , CO, CO_2 , and CH_4 in the thermal degradation of anionic gum. However, due to variations in structure and functional groups, both the degradation pathways and the resulting fragments can differ [26].

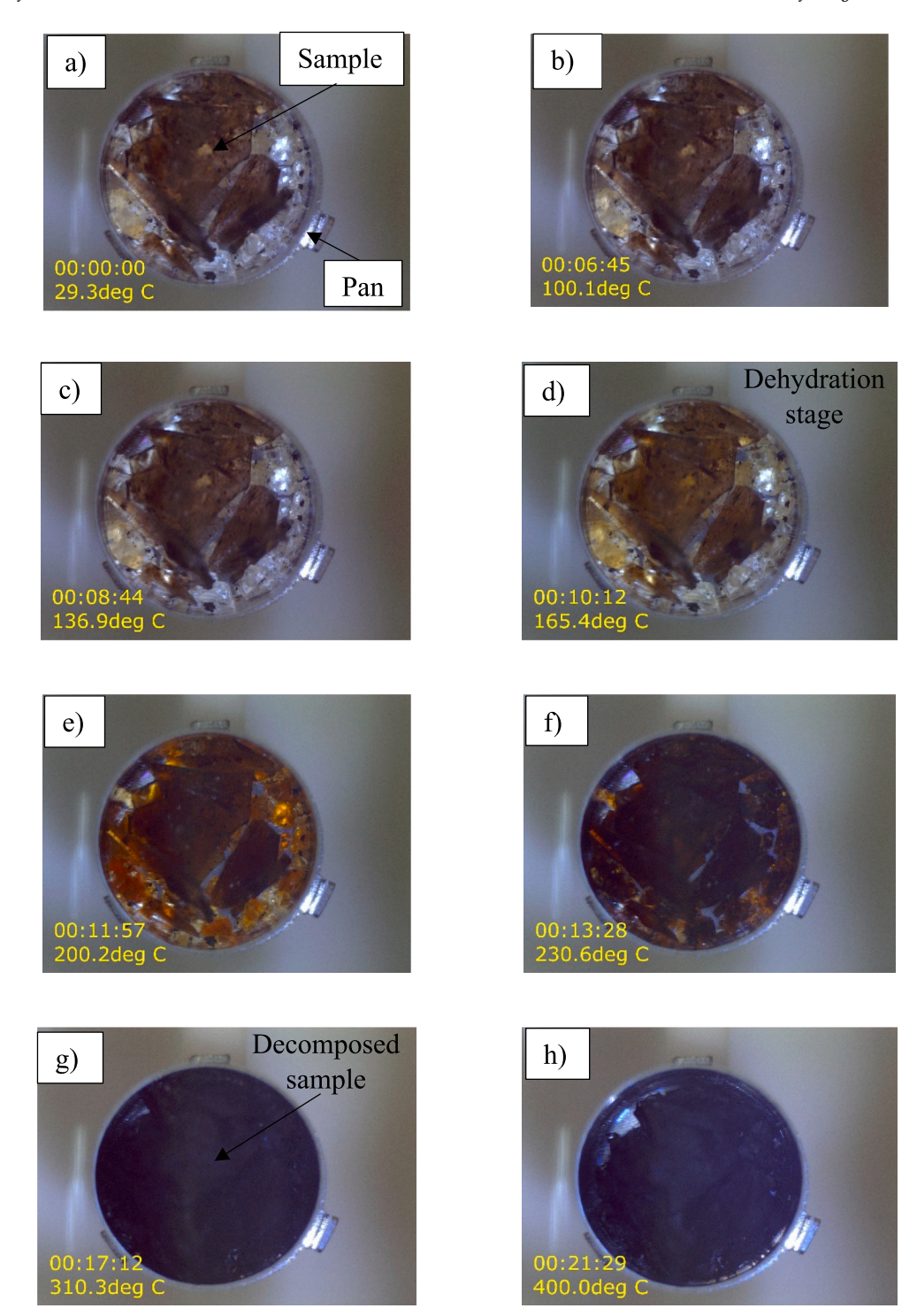


Fig. 4. Images taken at different temperatures (a) first image at start (b) image at 100 °C (c) image at first endothermic peak (d) color change starts (e) image at 200 °C (f) complete color change to black (g) image at first exothermic peak (h) last image at 400 °C.

3.3. Differential scanning calorimetry

Differential Scanning Calorimetry (DSC) serves as a fundamental technique for assessing the thermal properties of materials, establishing a correlation between temperature and specific physical characteristics. The DSC thermograms of the cashew gum sample are depicted in Fig. 2, revealing both endothermic (heat absorption) and exothermic (heat liberation) peaks at 100 $^{\circ}\text{C}$ - 194 $^{\circ}\text{C}$ and 335 $^{\circ}\text{C}$, respectively. The endothermic transition is associated with the dehydration of water from the gum, involving the removal of loosely bound water, such as

hydrogen-bonded or physically adsorbed water. The broad nature of the endothermic peak suggests a less organized packing of cashew gum [13]. In essence, the absence of a sharp endothermic peak confirms the amorphous nature of cashew gum, indicating its non-semi-crystalline nature. The first endotherm in the thermogram of cashew gum at 57.95 °C can be attributed to the enthalpy relaxation of the polymer [28]. As per Horvat et al., the second endotherm was attributed to the polymer's melting [29]. Olorunsola et al. [22] reported the melting point of cashew gum at 305 °C with an enthalpy change of 286.36 J/g, while Mothé and De Freitas [9] identified a degradation range of 245 °C

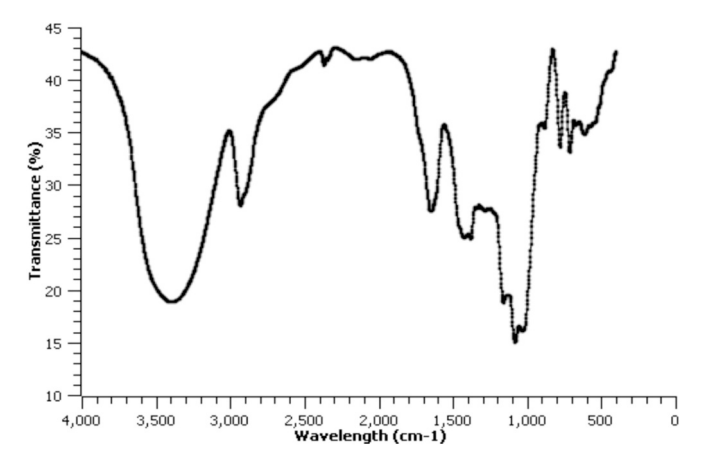


Fig. 5. FTIR spectrum of cashew gum.

Table 1Absorption bands and their relevant origin for the graph observed from FTIR spectrum.

Absorption	Bands [33]	Origin
3800–3000 cm ⁻¹	Phenolic OH stretching	Cellulosic material [34]
2929 cm^{-1}	CH ₂ asymmetrical stretching	Aliphatic bonds [34]
2365–2050 cm ⁻¹	$C \equiv C \text{ bond}$	Hemicellulose and lignin
1645 cm ⁻¹	C=O stretching of unsaturated ketone	Lignin bonds [34]
1424 cm^{-1}	CH in-plane deformation	Lignin bonds [35]
$1378~{\rm cm}^{-1}$	Phenol or tertiary alcoholic OH bending	Cellulose, hemicellulose and lignin [35]
$1158~{\rm cm}^{-1}$	C-O-C asymmetrical stretching	Cellulose and hemicellulose [35]
$1081~{\rm cm}^{-1}$	C-O stretching vibrations for ester	Cellulose and hemicellulose [35]
$1030~{\rm cm}^{-1}$	C-O, C=C, C-C-O stretching for alkoxy	Cellulose, hemicellulose and lignin [34]
870–700 cm ⁻¹	Aromatic C—H out of plane bending	Hemicellulose [35]
690–600 cm ⁻¹	Aromatic OH out of plane bending	

to 360 °C, with a maximum enthalpy change of 151.4 °C. Notably, Olorunsola et al. [22] did not observe an exothermic degradation range, and Mothé and De Freitas [9] did not identify an endothermic melting point. However, the current study concludes that cashew gum lacks a distinct melting point, as explained in Section 3.4. Additionally, a diffuse exothermic transition was observed post 288.51 °C, with its peak at 315.48 °C, signifying clear polymer degradation [30]. Just like most polysaccharides, cashew gum also experienced an exothermic transition of degradation. The observed enthalpy change of 382 J/g indicates the loss of 382 J of heat as 1 g of the polymer undergoes degradation. The occurrence of polymer degradation after melting could be attributed to the high inorganic composition of the polymer [31].

In the current investigation, the absence of detected exothermic curves suggest that, cashew gum lacks a crystal structure. Under certain conditions, when the appropriate temperature is reached post-relaxation, particles may orderly arrange themselves, leading to the formation of crystals in a process known as crystallization. Crystallization involves heat loss, making it an exothermic transition [29]. As it occurs at a constant temperature, it is considered a first-order reaction [32]. As heating continues beyond crystallization, a temperature is reached when the crystals move out of the orderly arrangement in a process called melting. Just like crystallization, melting takes place at a constant temperature. It is thus a first-order transition [29]. It can be concluded that when this polymer was heated, it was converted from the

amorphous to pseudo amorphous form in the process of enthalpy relaxation. Enthalpy relaxation is characterized by an endothermic process, signifying the absorption of heat by the system. This process is linked to a rise in temperature, resulting in a change in heat capacity, making it a second-order reaction. Further heating resulted in polysaccharide breakdown reflected by the exothermic transition.

3.4. Simultaneous thermal analysis (STA)

The TG-DTA curve closely mirrors the individual TGA (as discussed in Section 3.2) and DSC (as discussed in Section 3.3) analyses, providing robust support for the previously derived results and corresponding conclusions. The curve distinctly portrays the sequential processes of dehydration and decomposition undergone by cashew gum upon heating, with no discernible melting point evident. This fact can be observed form Video 1 attached with the manuscript which has been recorded throughout the experimental period. The incorporation of a camera within the chamber allows real-time observation of these changes. Dehydration observed within the temperature range of 120 °C to 160 °C, while decomposition takes place in the temperature range of 340 °C to 380 °C, as depicted in Fig. 3. Additionally, the graph enables the identification of a temperature range where a rapid transformation occurs. facilitating the differentiation of phase changes. Fig. 4 illustrates key images depicting the transformations observed in TG-DTA analysis at various temperatures.

3.5. Fourier transform infra-red spectrometry analysis

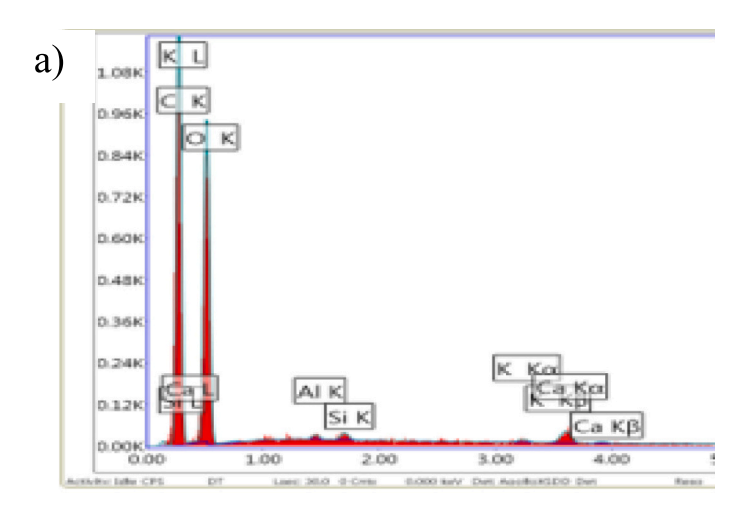
To discern the chemical bonds within a molecule, Fourier Transform Infrared Spectroscopy (FTIR) is employed to generate the infrared absorption spectrum as shown in Fig. 5. This resulting molecular fingerprint facilitates the examination of various compounds present in the sample. The region spanning $1500-500~\rm cm^{-1}$, known as the fingerprint region, is distinctive for each sample, while the region from 4000 to $1500~\rm cm^{-1}$ is designated as the functional group region. The cashew gum sample was tested in powder form added with KBr. Table 1 shows the complete breakdown of peaks and their respective origin sources.

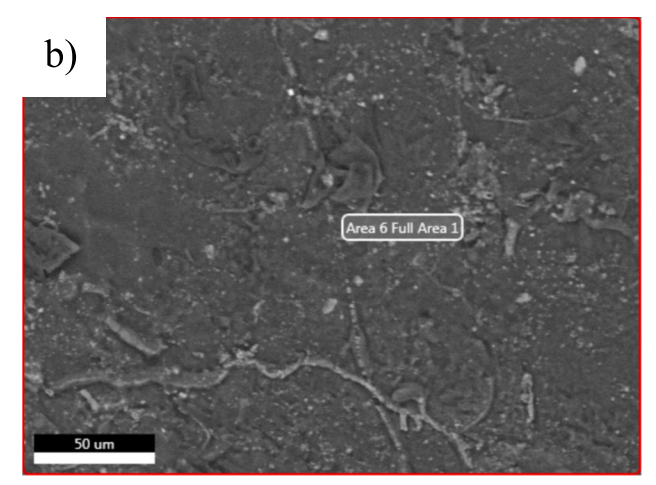
3.6. Scanning electron microscope and energy dispersive X-ray analysis

Fig. 6 (a)-(c) illustrate the SEM-EDX diagrams of cashew gum, revealing higher amounts of carbon and oxygen, as well as trace amounts of aluminum, silicon, potassium, and calcium. SEM/EDX is adept at surface analysis, making it well-suited for examining surface composition and elemental mapping. This technique employs an electron beam to excite the sample, leading to the emission of characteristic X-rays. SEM/EDX is particularly effective for elements with low atomic numbers (below 20) due to the electron beam's efficient interaction with their electronic structures, inducing X-ray emissions. The method generally exhibits a lower detection limit for light elements, enhancing sensitivity in the analysis of low atomic number elements like carbon, nitrogen, oxygen, and fluorine.

3.7. Micro X-ray fluorescence test

Performing μ -XRF alongside SEM/EDX is considered a complementary analysis, and they are not mutually exclusive alternatives. SEM/EDX is proficient in clearly identifying nonmetals and elements with atomic numbers below 20. Conversely, μ -XRF utilizes X-rays to excite the sample and measures the emitted characteristic X-rays for element identification. It is particularly effective for elements with higher atomic numbers (above 20) due to the more prominent and easily detectable X-ray emissions. XRF generally exhibits a higher detection limit for light elements compared to SEM/EDX and is more sensitive to elements with higher atomic numbers, such as transition metals and heavy elements. XRF can offer elemental analysis of both the surface and bulk of the





Element	Weight (%)	Atomic (%)
C K	33.6	41.02
ΟK	62.72	57.48
AlK	0.35	0.19
SiK	0.56	0.29
KK	0.49	0.19
CaK	2.28	0.83

Fig. 6. (a) The elemental spectrum (b) SEM diagram and (c) Percentage wise elements obtained for cashew gum using SEM/EDAX.

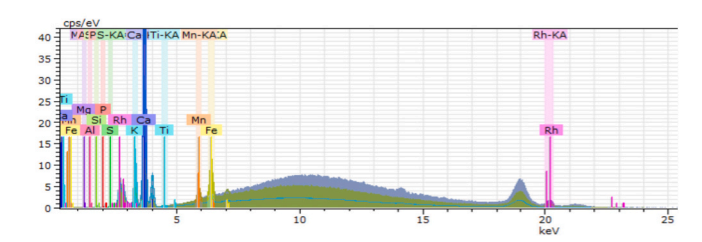


Fig. 7. μ-XRF spectrum obtained for cashew gum.

Table 2 Elements observed in cashew gum using μ -XRF.

Element	AN	[wt%]	[norm. wt%]
Magnesium	12	0.31	9.82
Aluminum	13	0.08	2.65
Silicon	14	0.1	3.08
Sulfur	16	0.01	0.43
Potassium	19	0.59	18.23
Calcium	20	1.42	44.21
Titanium	22	0.02	0.71
Manganese	25	0.19	5.91
Iron	26	0.48	14.96
		3.20	100

sample, making it suitable for comprehensively studying the material's overall composition. The spectrum obtained for $\mu\text{-XRF}$ analysis is shown in Fig. 7 and the elements present are featured percentage wise in Table 2.

3.8. Determination of micro hardness

In micro hardness testing, as the indenter penetrates the surface of the samples, they undergo deformation, counteracting the load applied by the indenter. Thus, Fig. 8 illustrates the load versus depth curves during indentation. The maximum depths reached during the experimental procedure for cashew gum samples were approximately 8300 ± 251 . 47 nm. The obtained hardness value for cashew gum in this research is 218.39 ± 14 MPa, falling within a comparable range to experiments conducted on epoxy resin (E51) with furan-based amine curing agents benzene methane-2,2-di (2-furylmethylamine) (BDFA) and epoxy resin (E51) with propane-2,2-di (2-furylmethylamine) (PDFA) [37]. E51/PDFA yielded 246 ± 5 MPa, and E51/BDFA yielded 267 ± 9 MPa, with maximum indentations of 1336 nm and 1281 nm, respectively [36]. However, the hardness obtained for cashew gum in this research is 1.6 times lower than the hardness of cured polyester resin (Hardness = 392 MPa) [37].

3.9. Determination of tensile strength

The tensile test is a fundamental mechanical assessment employed to

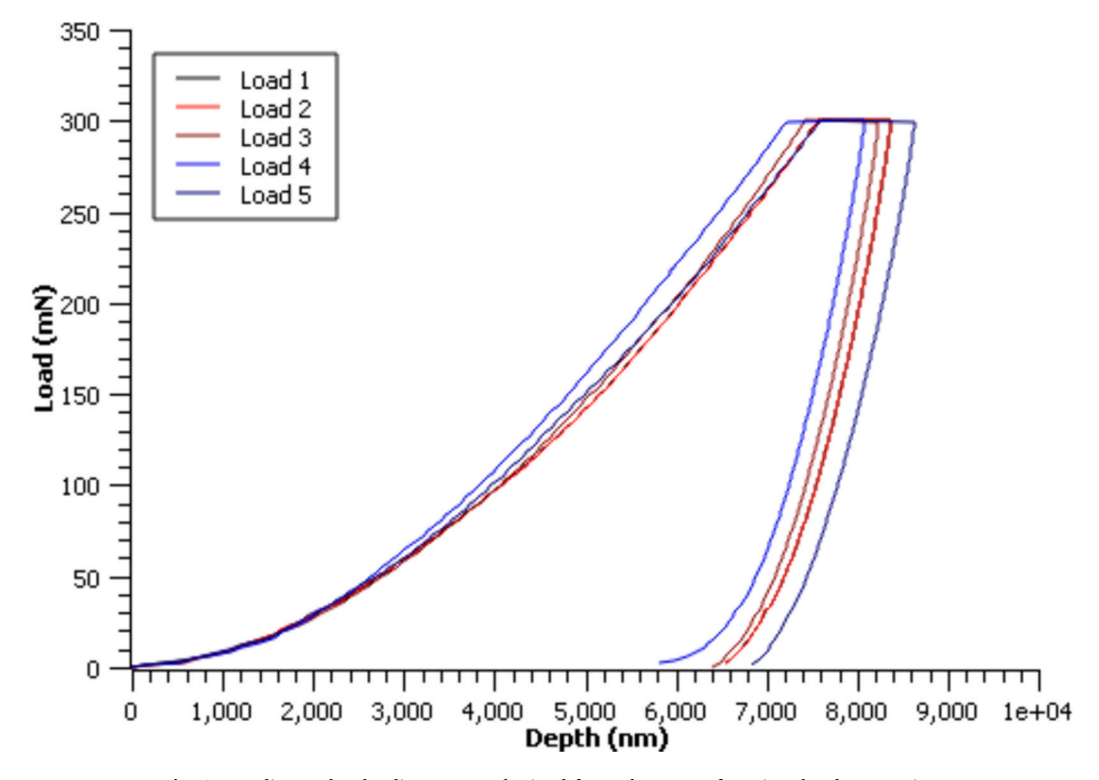


Fig. 8. Loading and unloading curves obtained for cashew gum for micro hardness testing.

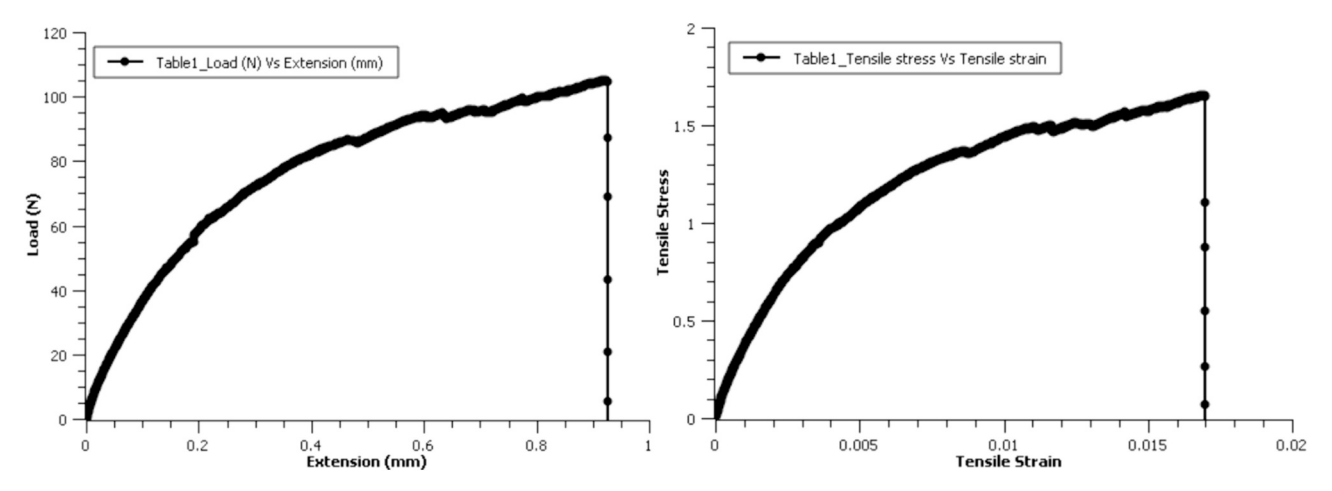


Fig. 9. (a) Load vs. extension and (b) stress vs. strain graphs obtained under tensile test.

Table 3Results obtained from tensile test.

Maximum Load	Maximum Tensile stress	Modulus (Automatic Young's)	Tensile extension at Maximum Load
(N)	(MPa)	(MPa)	(mm)
104.81 ± 16.8	1.67 ± 0.53	495.8 ± 45.32	0.93 ± 0.025

determine the mechanical properties of materials under axial loading. In this test, the specimen undergoes a gradually increasing axial force until it experiences deformation and ultimate failure. Tensile testing was conducted on cashew gum to obtain mechanical properties, including ultimate tensile strength and elastic modulus. The variations in ultimate tensile strength and yield strength for the composite specimen are

depicted in Fig. 9 and the results are mentioned in Table 3. The tensile test revealed an ultimate tensile strength of 1.6673 \pm 0.53 MPa, a Young's modulus of 495.79 \pm 45.32 MPa, and a percentage of elongation of 0.93 \pm 0.025. The tensile strength of cashew gum is attributed to hydrogen bonding and molecular interactions contributing to the formation of the hydration layer around suspended particles, without reducing surface and interfacial tension.

3.10. Determination of flexural test

The flexural modulus quantifies a material's stiffness when subjected to bending or flexural deformation, indicating its resistance to deformation under bending stress. This modulus is determined by analyzing the ratio of stress to strain in the elastic region of the stress-strain curve obtained from a flexural test. The variations in the flexural load vs. flexural extension and flexural strength vs. flexural strain of the

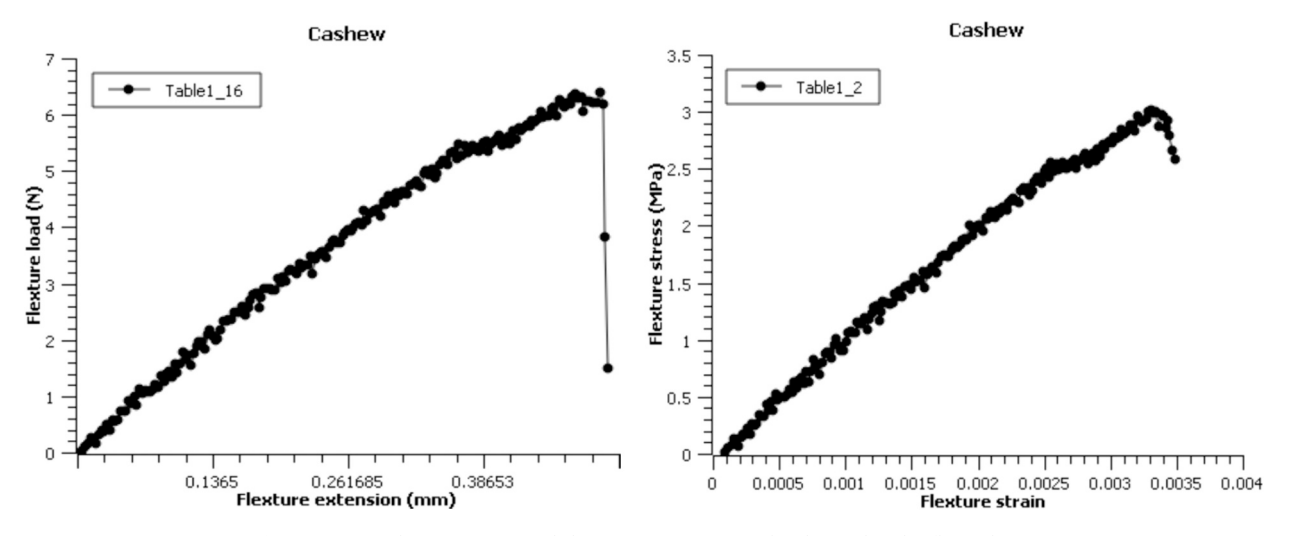


Fig. 10. (a) Load vs. extension and (b) stress vs. strain graphs obtained under flexural test.

Table 4
Results obtained from flexural test.

Maximum Flexure load	Flexure extension at Maximum Flexure load	Flexure strain at Maximum Flexure load	Flexure stress at Maximum Flexure load	Modulus (Automatic Young's)
(N)	(mm)	(mm/mm)	(MPa)	(MPa)
7.49 ± 0.6	0.58 ± 0.133	$0.004 \pm 2.64 \\ \times 10^{-4}$	3.64 ± 0.037	$1472. \pm \\ 0.141$

composite specimen are illustrated in Fig. 10. The flexural strength, flexural extension, flexural strain, and flexural modulus observed during the flexural test for the cashew gum sample were 3.64 \pm 0.037 MPa, 0.58 \pm 0.133 mm, 0.004 \pm 2.64 \times 10 $^{-4}$, and 1.472 \pm 0.141 GPa, respectively, as depicted in Table 4.

3.11. Determination of compressive strength

The compression test is a mechanical testing method employed to evaluate a material's capacity to endure axial loads that aim to compress it. The variations in the composite specimen's compressive load vs.

compressive extension and compressive strength vs. compressive strain are illustrated in Fig. 11. During the compressive test, a maximum compressive strength of 2.6673 ± 0.0161 MPa and a compressive strain of 0.55 ± 0.025 were obtained as can be seen from Table 5. The maximum load applied for 50 % compression was 520.92 ± 21.96 N.

3.12. Viscosity

Fig. 12 illustrates the reduction in viscosity as temperature increases, a phenomenon commonly observed in various liquids. Galmarini et al. mentioned that, with the increase of temperature, the viscosity of guar

Table 5Results obtained from compression test.

Maximum Compressive load	Compressive extension at Maximum Compressive load	Compressive strain at Maximum Compressive load	Compressive stress at Maximum Compressive load
(N)	(mm)	(mm/mm)	(MPa)
520.92 ± 21.96	15.00	0.55 ± 0.025	2.66 ± 0.0161

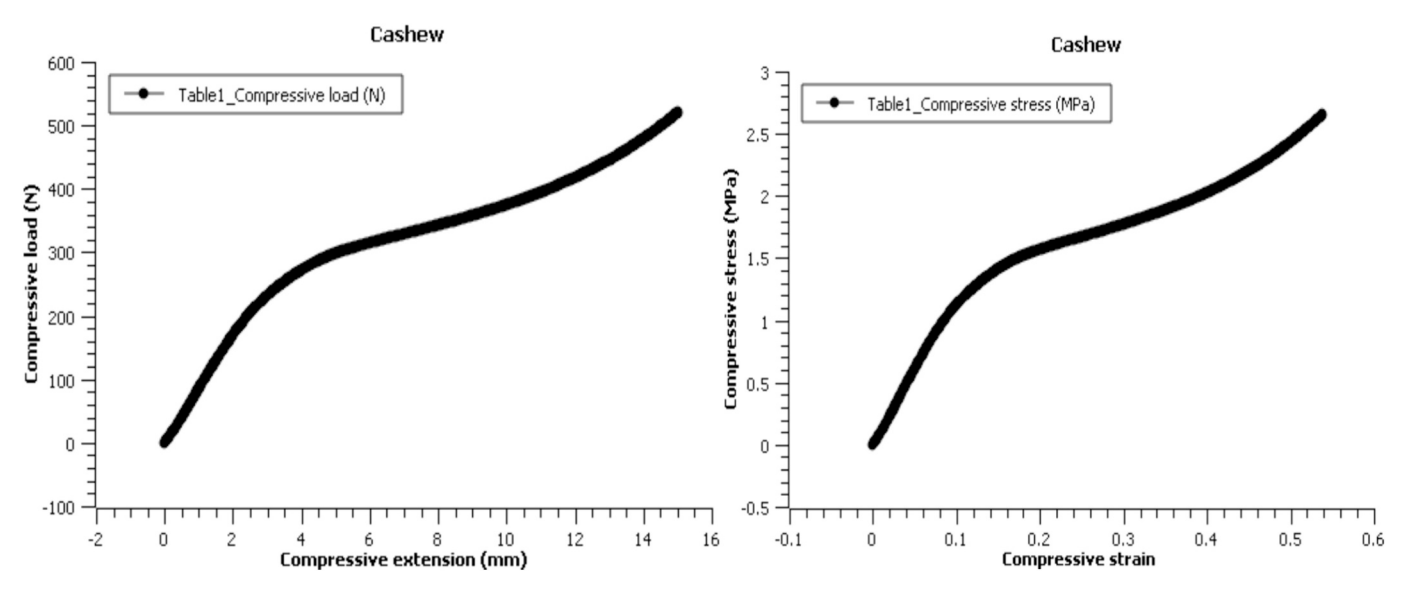


Fig. 11. (a) Load vs. extension and (b) stress vs. strain graphs obtained under tensile test.

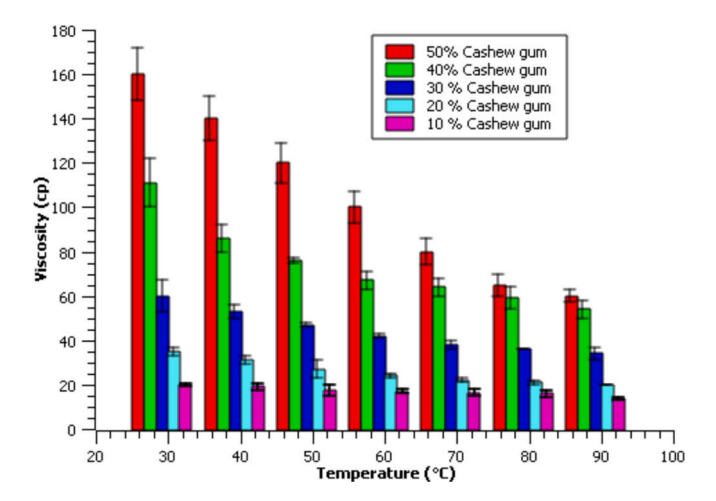


Fig. 12. Viscosity variation of cashew gum with increasing temperature and % cashew gum mixture.

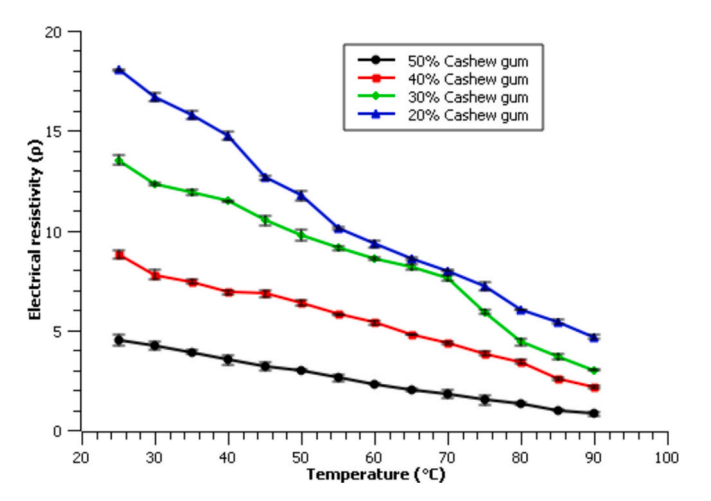


Fig. 13. Change of electrical resistivity of cashew gum with temperature and concentration.

gum added trehalose and sucrose decreases [38]. Chaudhari & Annapure also tested the viscosity of acacia gum and limonia acidissima L gum and found that, the viscosity increases with the increase of concentration of gums and decreases with the increase in temperature [39]. Kar & Arslan also mentioned such a similar trend regarding the dependence of viscosity on temperature and concentration [40]. Natural plant gums often contain large, complex polymers that, at higher concentrations, tend to become entangled with each other. This entanglement restricts the movement of individual polymer chains, resulting in increased viscosity. Controlling and understanding the viscosity of plant gum solutions is crucial in various industries, including food, cosmetics, and pharmaceuticals, where these natural polymers serve as common thickeners, stabilizers, or gelling agents.

3.13. Electrical resistivity

The relationship between the electrical resistivity of the gum and both temperature and gum concentration are depicted in Fig. 13. The graph illustrates that as the concentration and temperature of the gum increase, the electrical resistivity decreases. In the cashew gum sample, ions act as charge carriers, and the increase in their concentration results in reduced electrical resistivity, as a higher quantity of charge carriers supports conductivity. Bhakat et al. also mentioned that, conductivity of their research samples increases with increasing gum arabic content

Comparison of the properties of cashew gum with other artificial resins.

Polymer matrix	LDPE	HDPE	PP	PET	PLA	PHA	Phenolic resin	Epoxy resin	Polyester resin	Vinyl ester resin	Cashew gum
Density (g/cm ³)	0.91-0.93	0.94-0.96	0.84-0.92	1.3–1.4	1.21-1.29	1	1.21-1.32	1.1–1.4	1.11	1.03-1.15	1.36
Tensile strength (MPa)	5–25	15-40	25-40	22	49.6–72	17-40	45	35–37	33–85	70–80	1.66
Tensile modulus (GPa)	0.1-0.3	0.5-1.3	0.9-2	2.7-7.2	2.7–16	0.2 - 3.5	6.5	3–6	3.2–3.9	3-3.8	0.495
Elongation at break (%)	190-400	150-380	80	100-250	2.4-6	2–680	1.2-2	1–6	1.5-5	4-6	1.84
Strain at yield (%)	19	8.7-15	7-12	4	2.4-10	ı	1	4	1	4.85 ± 0.59	1.7
Flexural strength (MPa)	7.5	ı	41	88-78	83	ı	76-120	48.65-325	40.6–113	60–163	3.64
Flexural modulus (GPa)	0.23 - 0.495	0.75 - 1.6	1.24-1.6	1.56-2.65	1-3.8	ı	1	1.26 - 15.5	1.53-4.6	3.2-4.2	1.47
Compressive strength (MPa)	ı	20	40	80	1	1	1	116-404	104-131	82	2.66
Melting Temperature (°C)	106-115	120 - 180	120-176	245–265	164-178	45–54	1	90–245	1	ı	ı
Decomposition Temperature (°C)	1	250<	328	285–329	200<	ı	1	1	ı	ı	316

LDPE - low density polyethylene, HDPE - high density polyethylene, PP - poly propylene, PET - poly ethylene tetraphthalate, PLA - poly lactic acid, PHA - poly hydroxy alkanoate.

[41]. Amorim et al. supported this statement for some extent while testing for the electrical conductivity of polyaniline blended cashew gum samples saying that, the electrical conductivity increases with increasing cashew gum concentration up to 20 % (*w*/*w*) beyond which it decreased since cashew gum was acting as a dispersing agent [42].

3.14. Comparison of the properties of cashew gum with other artificial resins

The results obtained are compared with certain properties of artificial resins, providing valuable insights into the similarities and differences between natural and synthetic materials. This comparative analysis enhances the understanding of cashew gum's characteristics and its potential applications. It is used in pharmaceutical industry as binding agent of capsules due to its high viscosity under low temperature. It can also be used as a cap to cutting tools like drill bits after manufacturing - during transportation to protect its sharp edges from any possible damages. It can also be used as electrical insulations since it has a higher resistivity under low temperature. Table 6 shows the comparison of different properties of various artificial resins extracted from various research works [37,43-54]. It can be noticed that, many properties of cashew gum including flexural modulus, tensile modulus, density, and decomposition temperature can be compared with artificial resins. Further analysis may yield a path for the application of cashew gum as a better binding agent or matrix while using it in adhesive industries.

4. Conclusions

This study aimed to comprehensively characterize the thermal, chemical and mechanical properties of cashew gum (Anacardium occidentale tree gum) through a variety of analytical techniques. The pH of cashew gum was determined to be 4.76. Thermo Gravimetric Analysis (TGA) revealed distinct stages in the thermal behavior of cashew gum, corresponding to moisture evaporation and the decomposition of hemicellulose, cellulose, and lignin. The decomposition profile provided crucial insights into the thermal stability of cashew gum. Differential Scanning Calorimetry (DSC) analysis unveiled thermal transitions, showcasing endothermic peaks related to dehydration and exothermic peaks associated with polymer degradation. The absence of sharp endothermic peaks indicated the amorphous nature of cashew gum, confirming the lack of a crystal structure and, consequently, a melting point as demonstrated by TG-DTA analysis. Fourier-Transform Infrared (FTIR) spectra highlighted key absorption bands, aiding in the identification of specific chemical bonds and providing a molecular fingerprint for the gum. Surface analysis through Scanning Electron Microscopy with Energy Dispersive X-ray Analysis (SEM/EDAX) and micro-X-ray fluorescence (µ-XRF) unveiled the elemental composition of cashew gum, emphasizing the presence of carbon, oxygen, and trace amounts of other elements such as aluminum, magnesium, potassium, and calcium. In terms of mechanical properties, the micro hardness test indicated a hardness of 238.64 MPa for cashew gum, aligning with comparable studies on resin materials. Furthermore, the tensile strength, flexural strength, and compressive strength of cashew gum were determined to be 1.0155 MPa, 1.899 MPa, and 1.1023 MPa, respectively. The collective results from these analyses contribute to a comprehensive understanding of cashew gum, providing valuable data for researchers and industries exploring its applications across various fields. The diverse array of analytical techniques ensures a thorough characterization of cashew gum from thermal, chemical, and mechanical perspectives.

Supplementary data to this article can be found online at $\frac{https:}{doi.}$ org/10.1016/j.ijbiomac.2024.132396.

Formatting of funding sources

This research did not receive any specific grant from funding

agencies in the public, commercial, or not-for-profit sectors.

CRediT authorship contribution statement

Jebaratnam Joy Mathavan: Writing – original draft, Methodology, Investigation, Formal analysis, Conceptualization. **Muhammad Hafiz bin Hassan:** Writing – review & editing, Validation, Supervision, Conceptualization.

Declaration of competing interest

The authors declare that they have no known competing financial interests or personal relationships that could have appeared to influence the work reported in this paper.

Data availability

No data was used for the research described in the article.

Acknowledgement

The authors would like to thank the facility and technical support from the School of Mechanical Engineering, Universiti Sains Malaysia.

References

- I.J. Ogaji, E.I. Nep, J.D. Audu-Peter, Advances in natural polymers as pharmaceutical excipients, Pharmaceutica Analytica Acta (2012) 1–16.
- [2] K. Ofori-Kwakye, Y. Asantewaa, S.L. Kipo, Physicochemical and binding properties of cashew tree gum in metronidazole tablet formulations, Int J Pharm Pharm Sci 2 (Suppl. 4) (2010) 105–109.
- [3] J. Muñoz, et al., Rheological properties and surface tension of Acacia tortuosa gum exudate aqueous dispersions, Carbohydr. Polym. 70 (2) (2007) 198–205, https:// doi.org/10.1016/j.carbpol.2007.03.018.
- [4] R. da Silveira Nogueira Lima, J. Rabelo Lima, C. Ribeiro de Salis, R. de Azevedo Moreira, Cashew-tree (Anacardium occidentale L.) exudate gum: a novel bioligand tool, Biotechnol. Appl. Biochem. 35 (1) (2002) 45, https://doi.org/10.1042/ ba20010024.
- [5] R.C.M. de Paula, J.F. Rodrigues, Composition and rheological properties of cashew tree gum, the exudate polysaccharide from Anacardium occidentale L, Carbohydr. Polym. 26 (1995) 177–181.
- [6] G.L. De Pinto, M. Martinez, J.A. Mendoza, E. Ocando, C. Rivas, Comparison of three anacardiaceae gum exudates, Biochem. Syst. Ecol. 23 (2) (1995) 151–156, https://doi.org/10.1016/0305-1978(95)93848-W.
- [7] E.I. Okoye, A.O. Onyekweli, F.O. Ohwoavworhua, O.O. Kunle, Comparative study of some mechanical and release properties of paracetamol tablets formulated with cashew tree gum, povidone and gelatin as binders, Afr. J. Biotechnol. 8 (16) (2009) 3970–3973.
- [8] V.D. Alves, et al., Effect of temperature on the dynamic and steady-shear rheology of a new microbial extracellular polysaccharide produced from glycerol byproduct, Carbohydr. Polym. 79 (4) (2010) 981–988, https://doi.org/10.1016/j. carbool.2009.10.026.
- [9] C.G. Mothé, J.S. De Freitas, Thermal behavior of cashew gum by simultaneous TG/DTG/DSCFT-IR and EDXRF, J. Therm. Anal. Calorim. 116 (3) (2014) 1509–1514, https://doi.org/10.1007/s10973-014-3788-1.
- [10] Atul Tiwari; Baldev Raj, Reactions and Mechanisms in Thermal Analysis of Advanced Materials. Scrivener Publishing LLC. doi:https://doi.org/10.1002/ 9781119117711.
- [11] T.R. Crompton, Thermal Methods of Polymer Analysis. Smithers Rapra Technology.
- [12] P. K. G. Michael E. Brown, "Introduction to recent advances, techniques and applications of thermal analysis and calorimetry," in Handbook of Thermal Analysis and Calorimetry, 1st Editio., P. K. G. Michael E. Brown, Ed., Elsevier B.V., pp. 1–12.
- [13] R.M.A. Daoub, A.H. Elmubarak, M. Misran, E.A. Hassan, M.E. Osman, Characterization and functional properties of some natural Acacia gums, J. Saudi Soc. Agric. Sci. 17 (3) (2018) 241–249, https://doi.org/10.1016/j. issas.2016.05.002.
- [14] T.O. Chandra, et al., Tensile properties of epoxy resin filled with activated carbon derived from coconut shell, Mater Today Proc 66 (2022) 2967–2971, https://doi. org/10.1016/j.matpr.2022.06.568.
- [15] B.A. Mebratie, B.S. Ayele, A.A. Meku, Investigating the tensile and flexural strength of sunflower oil treated Ethiopian Highland bamboo fibre reinforced polyester composites, Advances in Bamboo Science (2023) 100021, https://doi.org/ 10.1016/j.bamboo.2023.100021.
- [16] R. Karthikeyan, R. Girimurugan, G. Sahoo, P. Maheskumar, A. Ramesh, Experimental investigations on tensile and flexural properties of epoxy resin matrix

- waste marble dust and tamarind shell particles reinforced bio-composites, Mater Today Proc 68 (2022) 2215–2219, https://doi.org/10.1016/j.matpr.2022.08.435.
- [17] F. Nik Wan, et al., The flexural properties of oil palm trunk (OPT) impregnated with epoxy (OPTE) composite manufactured by vacuum-assisted resin transfer moulding (VARTM) technique, Eng. Fail. Anal. 147 (2023) 107127, https://doi. org/10.1016/j.engfailanal.2023.107127.
- [18] E. Eshun Oppong, N. Kuntworbe, Y. Asantewaa Osei, K. Ofori-Kwakye, O. Adi-Dako, E. Obese, Physicochemical characterisation of Piptadeniastrum africana (Hook. F.) gum, a potential pharmaceutical excipient, Sci Afr 13 (2021) e00925, https://doi.org/10.1016/j.sciaf.2021.e00925.
- [19] E.I. Nep, B.R. Conway, Characterization of Grewia gum, a potential pharmaceutical excipient, Journal of Excipients and Food Chemicals 1 (1) (2010) 30–40.
- [20] E. Gyedu-Akoto, et al., Physico-chemical properties of cashew tree gum, Afr. J. Food Sci. 2 (2) (2008) 60-64.
- [21] M. Halima, O. Ar, and and TS, "Studies on some physicochemical properties of Khaya senegalensis gum," Niger J. Pharm. Sci., vol. 7, pp. 147–153, Mar. 2008.
- [22] E.O. Olorunsola, P.G. Bhatia, B.A. Tytler, M.U. Adikwu, Thermochemical properties of hydrophilic polymers from cashew and Khaya exudates and their implications on drug delivery, J Drug Deliv 2016 (2016) 1–7, https://doi.org/ 10.1155/2016/7496585.
- [23] C. Di Blasi, Modeling chemical and physical processes of wood and biomass pyrolysis, Prog. Energy Combust. Sci. 34 (1) (2008) 47–90, https://doi.org/ 10.1016/j.pecs.2006.12.001.
- [24] A. Skreiberg, Ø. Skreiberg, J. Sandquist, L. Sørum, TGA and macro-TGA characterisation of biomass fuels and fuel mixtures, Fuel 90 (6) (2011) 2182–2197, https://doi.org/10.1016/j.fuel.2011.02.012.
- [25] H. Zhou, Y. Long, A. Meng, Q. Li, Y. Zhang, The pyrolysis simulation of five biomass species by hemi-cellulose, cellulose and lignin based on thermogravimetric curves, Thermochim. Acta 566 (2013) 36–43, https://doi.org/ 10.1016/j.tca.2013.04.040.
- [26] P.L.R. Cunha, J.S. Maciel, M.R. Sierakowski, R.C.M. De Paulaa, J.P.A. Feitosa, Oxidation of cashew tree gum exudate polysaccharide with TEMPO reagent, J. Braz. Chem. Soc. 18 (1) (2007) 85–92, https://doi.org/10.1590/S0103-50532007000100009.
- [27] W.-H. Chen, C.-W. Wang, H.C. Ong, P.L. Show, T.-H. Hsieh, Torrefaction, pyrolysis and two-stage thermodegradation of hemicellulose, cellulose and lignin, Fuel 258 (2019) 116168, https://doi.org/10.1016/j.fuel.2019.116168.
- [28] H.-J. Chung, E.-J. Lee, S.-T. Lim, Comparison in glass transition and enthalpy relaxation between native and gelatinized rice starches, Carbohydr. Polym. 48 (3) (2002) 287–298, https://doi.org/10.1016/S0144-8617(01)00259-4.
- [29] M. Horvat, E. Mestrović, A. Danilovski, D.Q.M. Craig, An investigation into the thermal behaviour of a model drug mixture with amorphous trehalose, Int. J. Pharm. 294 (1–2) (Apr. 2005) 1–10, https://doi.org/10.1016/j. iipharm.2004.08.025.
- [30] M.S. Iqbal, S. Massey, J. Akbar, C.M. Ashraf, R. Masih, Thermal analysis of some natural polysaccharide materials by isoconversional method, Food Chem. 140 (1–2) (2013) 178–182. https://doi.org/10.1016/j.foodchem.2013.02.047.
- [31] P.F. Builders, O.O. Kunle, M.U. Adikwu, Preparation and characterization of mucinated agarose: a mucin-agarose physical crosslink, Int. J. Pharm. 356 (1–2) (2008) 174–180, https://doi.org/10.1016/j.iipharm.2008.01.006.
- [32] P. Builders, C. Chukwu, I. Obidike, M. Builders, A. Attama, M. Adikwu, A novel xyloglucan gum from seeds of Afzelia africana Se. Pers.: some functional and physicochemical properties, International Journal of Green Pharmacy 3 (2) (2009) 112–118, https://doi.org/10.4103/0973-8258.54898.
- [33] J.L. White, Interpretation of infrared spectra of soil minerals, Soil Sci. 112 (1) (1971) 22–31, https://doi.org/10.1097/00010694-197107000-00005.
- [34] E. Lazzari, et al., Classification of biomass through their pyrolytic bio-oil composition using FTIR and PCA analysis, Ind. Crop. Prod. 111 (2018) 856–864, https://doi.org/10.1016/j.indcrop.2017.11.005.
- [35] F. Xu, J. Yu, T. Tesso, F. Dowell, D. Wang, Qualitative and quantitative analysis of lignocellulosic biomass using infrared techniques: a mini-review, Appl. Energy 104 (2013) 801–809, https://doi.org/10.1016/j.apenergy.2012.12.019.

- [36] M. Bu, X. Zhang, T. Zhou, C. Lei, Fully bio-based epoxy resins derived from magnolol and varying furan amines: cure kinetics, superior mechanical and thermal properties, Eur. Polym. J. 180 (2022) 111595, https://doi.org/10.1016/j. eurpolymi.2022.111595.
- [37] Polyester Resin, Hawley's Condensed Chemical Dictionary, 2007, https://doi.org/ 10.1002/9780470114735.hawley13103.
- [38] M.V. Galmarini, R. Baeza, V. Sanchez, M.C. Zamora, J. Chirife, Comparison of the viscosity of trehalose and sucrose solutions at various temperatures: effect of guar gum addition, LWT Food Sci. Technol. 44 (1) (2011) 186–190, https://doi.org/ 10.1016/i.lwt.2010.04.021.
- [39] B.B. Chaudhari, U.S. Annapure, Rheological, physicochemical, and spectroscopic characterizations of Limonia acidissima L. gum exudate with an application in extrusion processing, Carbohydrate Polymer Technologies and Applications 2 (2021) 100020, https://doi.org/10.1016/j.carpta.2020.100020.
- [40] F. Kar, N. Arslan, Effect of temperature and concentration on viscosity of orange peel pectin solutions and intrinsic viscosity-molecular weight relationship, Carbohydr. Polym. 40 (4) (1999) 277–284, https://doi.org/10.1016/S0144-8617 (99)00062-4
- [41] D. Bhakat, P. Barik, A. Bhattacharjee, Electrical conductivity behavior of gum Arabic biopolymer-Fe3O4 nanocomposites, J. Phys. Chem. Solids 112 (2018) 73–79, https://doi.org/10.1016/j.jpcs.2017.09.002.
- [42] D.R.B. Amorim, I. da Silva Guimarães, L. Fugikawa-Santos, M.L. Vega, H.N. da Cunha, Effect of temperature on the electrical conductivity of polyaniline/cashew gum blends, Mater. Chem. Phys. 253 (2020) 123383, https://doi.org/10.1016/j. matchemphys.2020.123383.
- [43] "Polymer Database." [Online]. Available: www.polymerdatabase.com.
- [44] S. Ramakrishnan, K. Krishnamurthy, R. Rajasekar, G. Rajeshkumar, An experimental study on the effect of nano-clay addition on mechanical and water absorption behaviour of jute fibre reinforced epoxy composites, J. Ind. Text. 49 (5) (Aug. 2018) 597–620, https://doi.org/10.1177/1528083718792915.
- [45] H.O. Van Quy, S.T.T. Nguyen, Experimental analysis of coir fiber sheet reinforced epoxy resin composite, IOP Conf Ser Mater. Sci. Eng. 642 (1) (2019), https://doi. org/10.1088/1757-899X/642/1/012007.
- [46] B. Coxworth, New Process Converts Old PLA Plastic Into a Better 3D-printing Resin, NEW ATLAS, 2022.
- [47] Encyclopedia Britannica, Polyethylene terephthalate, in: Britannica, The Editors of Encyclopaedia, 2023.
- [48] R. Zhao, P. Torley, P.J. Halley, Emerging biodegradable materials: starch- and protein-based bio-nanocomposites, J. Mater. Sci. 43 (9) (2008) 3058–3071, https://doi.org/10.1007/s10853-007-2434-8.
- [49] K. Sudesh, H. Abe, Y. Doi, Synthesis, structure and properties of polyhydroxyalkanoates: biological polyesters, Prog. Polym. Sci. 25 (10) (2000) 1503–1555, https://doi.org/10.1016/S0079-6700(00)00035-6.
- [50] A.P. Mathew, K. Oksman, M. Sain, Mechanical properties of biodegradable composites from poly lactic acid (PLA) and microcrystalline cellulose (MCC), J. Appl. Polym. Sci. 97 (5) (2005) 2014–2025, https://doi.org/10.1002/ app.21779.
- [51] W. Ouarhim, N. Zari, R. Bouhfid, A.E.K. Qaiss, Mechanical performance of natural fibers-based thermosetting composites, in: Mechanical and Physical Testing of Biocomposites, Fibre-Reinforced Composites and Hybrid Composites, 2018, pp. 43–60, https://doi.org/10.1016/B978-0-08-102292-4.00003-5.
- [52] S.P. Phifer, K.N.E. Verghese, J.J. Lesko, J. Haramis, Temperature-moisture-mechanical response of vinyl Ester resin and pultruded vinyl ester/E-glass laminated composites, in: JBT-PFA, P. Moalli (Eds.), Plastics Design Library, William Andrew Publishing, Norwich, NY, 2001, pp. 105–112, https://doi.org/10.1016/B978-188420792-1.50015-9.
- [53] H. Allen, DJ, Ishida, Thermosets: phenolics, novolacs, and benzoxazine, in: Encyclopedia of Materials: Science and Technology, 2001, pp. 9226–9229, https://doi.org/10.1016/b0-08-043152-6/01662-4.
- [54] G. Wypych, Handbook of Polymers, 2016, https://doi.org/10.1016/C2015-0-01462-9